npg

Feedback loops blockade potentiates apoptosis induction and antitumor activity of a novel AKT inhibitor DC120 in human liver cancer

F Yang[1,2,5], R Deng[1,5], X-J Qian[1,5], S-H Chang[3,4], X-Q Wu[1], J Qin[1], G-K Feng[1], K Ding*[,3,4] and X-F Zhu*[,1]

The serine/threonine kinase AKT is generally accepted as a promising anticancer therapeutic target. However, the relief of feedback inhibition and enhancement of other survival pathways often attenuate the anticancer effects of AKT inhibitors. These compensatory mechanisms are very complicated and remain poorly understood. In the present study, we found a novel 2-pyrimidyl-5-amidothiazole compound, DC120, as an ATP competitive AKT kinase inhibitor that suppressed proliferation and induced apoptosis in liver cancer cells both *in vitro* and *in vivo*. DC120 blocked the phosphorylation of downstream molecules in the AKT signal pathway in dose- and time-dependent manners both *in vitro* and *in vivo*. However, unexpectedly, DC120 activated mammalian target of rapamycin complex 1 (mTORC1) pathway that was suggested by increased phosphorylation of 70KD ribosomal protein S6 kinase (P70S6K) and eukaryotic translation initiation factor 4E binding protein 1 (4E-BP1). The activated mTORC1 signal was because of increase of intracellular Ca^{2+} via Ca^{2+}/calmodulin (CaM)/ signaling to human vacuolar protein sorting 34 (hVps34) upon AKT inhibition. Meanwhile, DC120 attenuated the inhibitory effect of AKT on CRAF by decreasing phosphorylation of CRAF at Ser259 and thus activated the mitogen-activated protein kinase (MAPK) pathway. The activation of the mTORC1 and MAPK pathways by DC120 was not mutually dependent, and the combination of DC120 with mTORC1 inhibitor and/or MEK inhibitor induced significant apoptosis and growth inhibition both *in vitro* and *in vivo*. Taken together, the combination of AKT, mTORC1 and/or MEK inhibitors would be a promising therapeutic strategy for liver cancer treatment.

Liver cancer is the fifth most frequently diagnosed cancer in men worldwide but the second most frequent cause of cancer death. In women, it is the seventh most commonly diagnosed cancer and the sixth leading cause of cancer death.[1] Liver cancer is well characterized as a highly refractory cancer with high levels of tumor progression and recurrence for which there is no effective systemic therapy yet. Intracellular signaling mitogen-activated protein kinase (MAPK) and phosphoinositide 3-kinase (PI3K)/AKT pathways have been recognized as important factors in liver cancer.[2]

AKT, also called protein kinase B (PKB), an evolutionarily conserved serine/threonine kinase, is the central regulator of the PI3K/AKT signaling pathway. Mammalian cells express three closely related isoforms (AKT1-3 or PKBα/β/γ) that are encoded by three separate genes, and AKT1 is well reported in various tissues.[3] AKT isoforms possess an N-terminal pleckstrin homology (PH) domain that mediates AKT recruitment to plasma membrane and induces conformational change that enables phosphorylation of Thr308 in AKT in the activation segment by membrane-localized 3-phosphoinositide-dependent kinase 1 (PDK1).[4] Phosphorylation of another residue Ser473 in AKT in the hydrophobic motif is required for maximal activity that is mediated by mammalian target of rapamycin (mTOR) complex 2 (mTORC2) consisting of Rictor, Sin1, mLST8, Protor 1 and Protor 2.[5] Once fully activated, AKT phosphorylates a variety of downstream substrates, such as forkhead protein family members (FOXO1, FOXO3α and AFX), proline-rich AKT substrate of

[1]State Key Laboratory of Oncology in South China, Collaborative Center for Cancer Medicine, Sun Yat-sen University Cancer Center, Guangzhou, China; [2]Department of Biochemistry and Molecular Biology, Nanjing Medical University, Nanjing, China; [3]Key Laboratory of Regenerative Biology and Institute of Chemical Biology, Guangzhou Institutes of Biomedicine and Health, Chinese Academy of Sciences, Guangzhou, China and [4]Graduate School, Chinese Academy of Sciences, Beijing, China
*Corresponding author: X-F Zhu, State Key Laboratory of Oncology in South China, Collaborative Center for Cancer Medicine, Sun Yat-sen University Cancer Center, 651 Dongfeng Road East, Guangzhou 510060, China. Tel: +86 20 87343149; Fax: +86 20 87343170; Fax: +86 20 32015299; E-mail: zhuxfeng@mail.sysu.edu.cn
or K Ding, Key Laboratory of Regenerative Biology and Institute of Chemical Biology, Guangzhou Institutes of Biomedicine and Health, Chinese Academy of Sciences, 190 Kaiyuan Avenue, Science Park, Guangzhou 510530, China; Graduate School, Chinese Academy of Sciences, 52 Sanlihe Road, Beijing 100864, China. Tel: +86 20 32015300; Fax: +86 20 32015299; E-mail: ding_ke@gibh.ac.cn.
[5]These authors contributed equally to this work.
Keywords: AKT inhibitor; apoptosis; MAPK pathway; mTOR complexes; PI3K/AKT pathway
Abbreviations: PKB, protein kinase B; PH, pleckstrin homology; GSK3β, glycogen synthetase kinase-3β; FOX, human forkhead box; mTOR, mammalian target of rapamycin; PRAS40, proline-rich AKT substrate of 40KD; PI3K, phosphoinositide 3-kinase; PIP3, phosphatidylinositol-3,4,5-trisphosphate; MAPK, mitogen-activated protein kinase; PIP2, phosphatidylinositol-3,4-bisphosphate; PDK1, 3-phosphoinositide-dependent kinase 1; TUNEL, transferase-mediated FITC-12-dUTP nick -end labeling; FKBP-12, FK506 binding protein 12; IRS-1, insulin receptor substrate-1; RTK, receptor tyrosine kinase; CaM, calmodulin; hVps34, human vacuolar protein sorting 34; TG, thapsigargin; BAPTA-AM, BAPTA-acetoxymethyl ester; EGTA, ethylene glycol bis(2-aminoethyl) tetraacetic acid; PARP, poly ADP-ribose polymerase; W7, N-(6-aminohexyl)-5-chloro-1-naphthalenesulfonamide; 3-MA, 3-methyladenine; ER, endoplasmic reticulum; Rheb, GTPase Ras homolog enriched in brain
Received 01.8.13; revised 22.12.13; accepted 17.1.14; Edited by M Piacentini

40KD (PRAS40), mTOR, glycogen synthetase kinase-3β (GSK3β), MDM2, Bad, tuberin/TSC2 and caspase-9.[6] AKT is also the most important regulator of mTOR complex 1 (mTORC1) that consists of mTOR, PRAS40, Raptor and mLST8 and is sensitive to the immunosuppressant and anticancer drug rapamycin.[7]

It becomes increasingly clear that intracellular Ca^{2+} signals controlling many vital cellular processes are confined to subcellular microdomains. Inositol 1,4,5-trisphosphate (IP3) receptor (IP3R) is a universal intracellular Ca^{2+}-release channel, the phosphorylation/dephosphorylation of which can regulate intracellular Ca^{2+} concentration and be involved in PI3K/AKT survival pathway. The IP3R is also a substrate for a wide variety of different protein kinases, such as PKA phosphorylating two distinct sites on IP3R1, PKG phosphorylating IP3R3 and IP3R1 phosphorylation by AKT inhibiting Ca^{2+} release.[8,9]

Currently, AKT is gradually accepted as a promising anticancer target and there are several types of small molecular AKT inhibitors available: ATP-competitive protein kinase inhibitors, such as GDC0068, GSK690693 and A-443654;[10–12] allosteric inhibitors, such as MK-2206;[13] and inhibitors of phosphatidylinositol-3,4,5-trisphosphate (PIP3) binding, such as perifosine.[14] Recently, many studies reported that AKT inhibitors could activate different feedback loops such as MAPK pathway and HER3 pathway dependent of cancer types. Activation of these feedback loops may significantly affect the efficacy of AKT inhibitors.[15,16] In the present study, a novel 2-pyrimidyl-5-amidothiazole compound DC120 (the structure seen in Figure 1a), which is an ATP-competitive AKT kinase inhibitor, was investigated. We found that DC120 inhibited phosphorylation of AKT downstream molecules and activated mTORC1 pathway via Ca^{2+}/calmodulin (CaM)/human vacuolar protein sorting 34 (hVps34) and MAPK pathway via decreasing the phosphorylation of C-Raf. Our results showed that the combination of an AKT inhibitor with mTORC1 inhibitor and/or MAPK inhibitor would be a promising therapeutic strategy for treatment of liver cancer.

Results

DC120 inhibited the activity of AKT kinase *in vitro*. Our previous study showed that the IC_{50} value of DC120 targeting AKT kinase was 0.153 μM in a cell-free system *in vitro* using an AKT Kinase Assay Kit.[17] To further investigate the selectivity of DC120 against AKT kinase, a large panel of kinases was tested by KINOMEscan, a division of DiscoveRx (Fremont, CA, USA). The compound was screened at the DC120 concentration of 0.1 and 1 μM, and the results for primary screening were reported as %Ctrl where lower numbers indicated stronger hits according to the DiscoveRx protocol. At 0.1 and 1 μM of DC120, the AKT1%Ctrl was 15 and 0.2, respectively, and the %Ctrl of other kinases was apparently greater than those in the corresponding concentration (Supplementary Table S1). However, different inhibitory effects of DC120 existed in AKT2 and AKT3 knockdown cells *versus* control cells (Supplementary Figure S1A and B). Thus, we declared that DC120 specifically inhibited AKT kinase activity, especially AKT1.

AKT, also named PKB, was highly homologous with PKA and PKC, and hence we determined the effects of DC120 on PKA and PKC kinases, and phosphorylation levels of PKA substrate CREB and PKC substrate c-Fos were detected. As shown in Supplementary Figure S1C, DC120 did not change phosphorylation levels of CREB and c-Fos, which suggested that DC120 had no obvious effects on PKA and PKC kinases. Moreover, %Ctrl of ADCK3, CSNK1D and DYRK1B in 1 μM of DC120 were also low, and thus correlation of DC120-induced inhibitory effects and these kinases was determined. As shown in Supplementary Figure S2, we found that the inhibitory effects of DC120 were similar in HepG2 and Bel7402 cells with ADCK3, CSNK1D and DYRK1B siRNA transfection compared with cells transfected with Ctrl siRNAs. This indicated that ADCK3, CSNK1D and DYRK1B kinases did not play roles in the inhibitory effects of DC120.

DC120 inhibited proliferation of liver cancer cells in AKT-dependent manner. To determine the effect of DC120 on cell proliferation, HepG2, SMMC7721, Bel7402 and Huh7 cells were exposed to DC120 at different concentrations ranging from 1.25 to 40 μM for 72 h, and a dose-dependent inhibition of cell viability was observed in all cell lines (Figure 1b). The IC_{50} values for HepG2, SMMC7721, Bel7402 and Huh7 cells were 10.43, 12.51, 7.73 and 13.32 μM, respectively. The IC_{50} value observed for the normal liver cell line LO2 was 62.99 μM, indicating that DC120 activity was obviously selective for liver cancer cells *versus* liver cells.

The dependency of inhibition of cell proliferation by DC120 on AKT activity was further investigated in HepG2 and Bel7402 cells. The results suggested that the reduction of AKT expression via shAKT markedly reduced the inhibitory effects of DC120 in HepG2 and Bel7402 cells (Figures 1c and d), which was similar to another new ATP- competitive inhibitor GDC0068 (Supplementary Figure S3). However, the inhibitory effects of DC120 increased significantly in HepG2 and Bel7402 cells upon PTEN knockdown (Figures 1e and f). These results indicated that the inhibition of liver cancer cells growth by DC120 depended on the activation of AKT, and cells with hyperactive AKT were more sensitive to DC120 than cells with normal AKT activity.

DC120 inhibited phosphorylation of AKT substrates and induced apoptosis. AKT functions in cell survival signaling by phosphorylating downstream targets, and dephosphorylation of these substrates indicates the inhibition of AKT activity. We thereby investigated whether DC120 could inhibit the phosphorylation of AKT substrates; as expected, the phosphorylation of FOXO3α and GSK-3β was reduced by DC120 in HepG2 and Bel7402 cells. Moreover, the phosphorylation of AKT Ser473 and Thr308 was elevated after treatment with DC120 (Figures 2a and b), consistent with the effects of A-443654 and GSK690693,[11,18] also similar to that of GDC0068 (Supplementary Figure S4).

HepG2 and Bel7402 cells were treated with the indicated concentrations of DC120, and apoptosis was evaluated. DC120 induced apoptosis in a dose-dependent manner. In cells treated with 20 μM DC120, apoptosis was increased
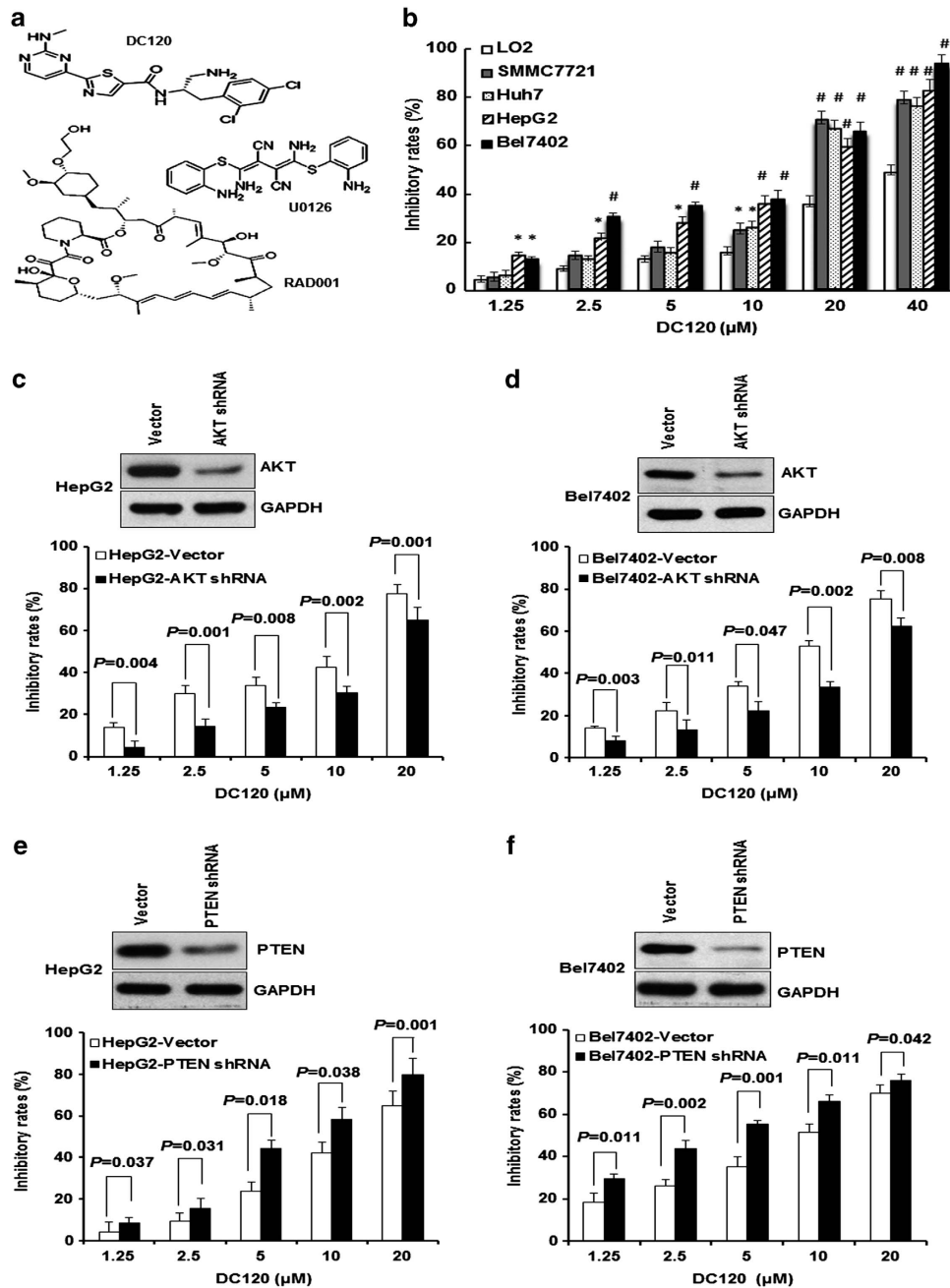
Figure 1 DC120 inhibited cell proliferation in an AKT-dependent manner. (**a**) The chemical structures of DC120, RAD001 and U0126. (**b**) The inhibitory effects of DC120 on liver cancer cells and normal liver cells LO2. $*P < 0.05$, $^{\#}P < 0.01$, inhibitory rates of four liver cancer cell lines *versus* LO2 cell line. (**c** and **d**) Knockdown of AKT decreased liver cancer cell sensitivity to DC120. Cells were stably transfected with plasmids loaded with empty vector or AKT shRNA, and then treated with indicated concentrations of DC120 for 72 h by MTT assay. (**e** and **f**) Knockdown of PTEN increased liver cancer cell sensitivity to DC120, as described in (**c** and **d**). The data shown are the means ± S.E. of three individual experiments

to 59.4% of cells in HepG2 and 53.6% in Bel7402 (Figure 2c). In addition, the proportion of cells in early apoptosis (%), as evaluated by Annexin V/PI staining, was increased to 14% in HepG2 cells and 28.7% in Bel7402 cells treated with the indicated concentration of DC120 (10 μM; Figure 2d). At 20 μM of DC120, the proportion of Annexin V/PI-double positive cells was increased to 75.8% in HepG2 and 67.3% in Bel7402. To further demonstrate that this cell death was due to apoptosis, caspase-3 and PARP expressions were

examined. As shown in Figure 2e, DC120 evidently induced the cleavages of caspase-3 and PARP in a dose-dependent manner.

DC120 activated the mTORC1 pathway and synergistically induced apoptosis with the mTORC1 inhibitor RAD001. Activated mTORC1 regulates the phosphorylation of 70KD ribosomal protein S6 kinase (P70S6K) and eukaryotic translation initiation factor 4E binding protein 1
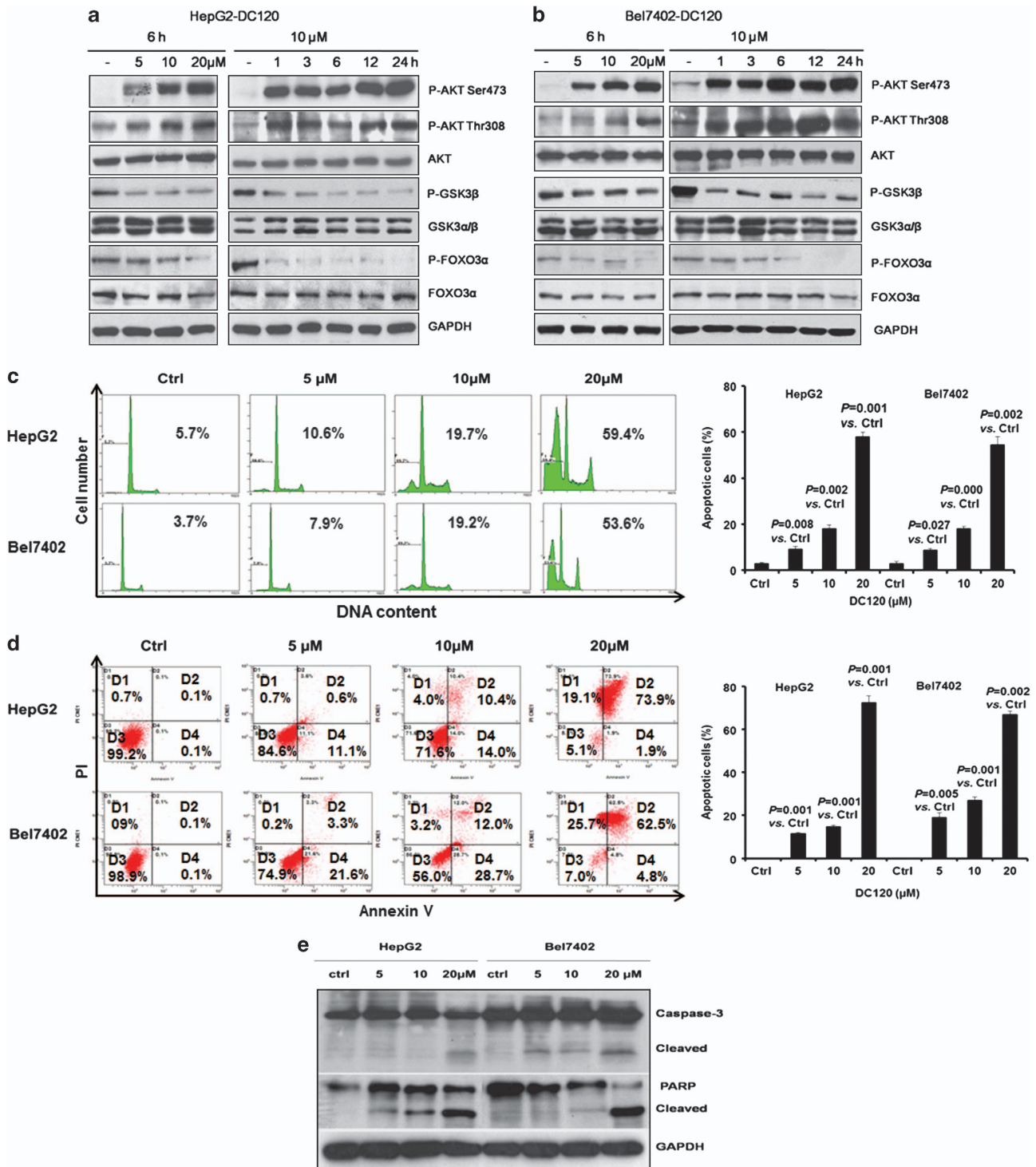
Figure 2 DC120 inhibited phosphorylation of AKT substrates and induced apoptosis. (**a** and **b**) DC120 inhibited the phosphorylation of GSK3β and FOXO3α but increased the phosphorylation of AKT at Ser473 and Thr308. (**c**) DC120 induced apoptotic cell death by PI staining (left panel as representative of three individual experiments, and the right panel as statistical analysis). (**d**) DC120-induced apoptotic cells were investigated by Annexin V/PI staining (the same as **c**). (**e**) DC120 induced markedly cleaved PARP and caspase-3. Cells were treated with DC120 for 48 h

(4E-BP1), the two main factors in mRNA translation and ribosome biogenesis, thus controlling the rate of protein synthesis.[19] To explore the effect of DC120 on the mTORC1 pathway, we detected the phosphorylation levels of mTOR,

P70S6K and 4E-BP1 and observed that DC120 attenuated the phosphorylation of mTOR but significantly increased the phosphorylation of P70S6K and 4E-BP1 (Figures 3a and b), which indicated that DC120 significantly stimulated mTORC1
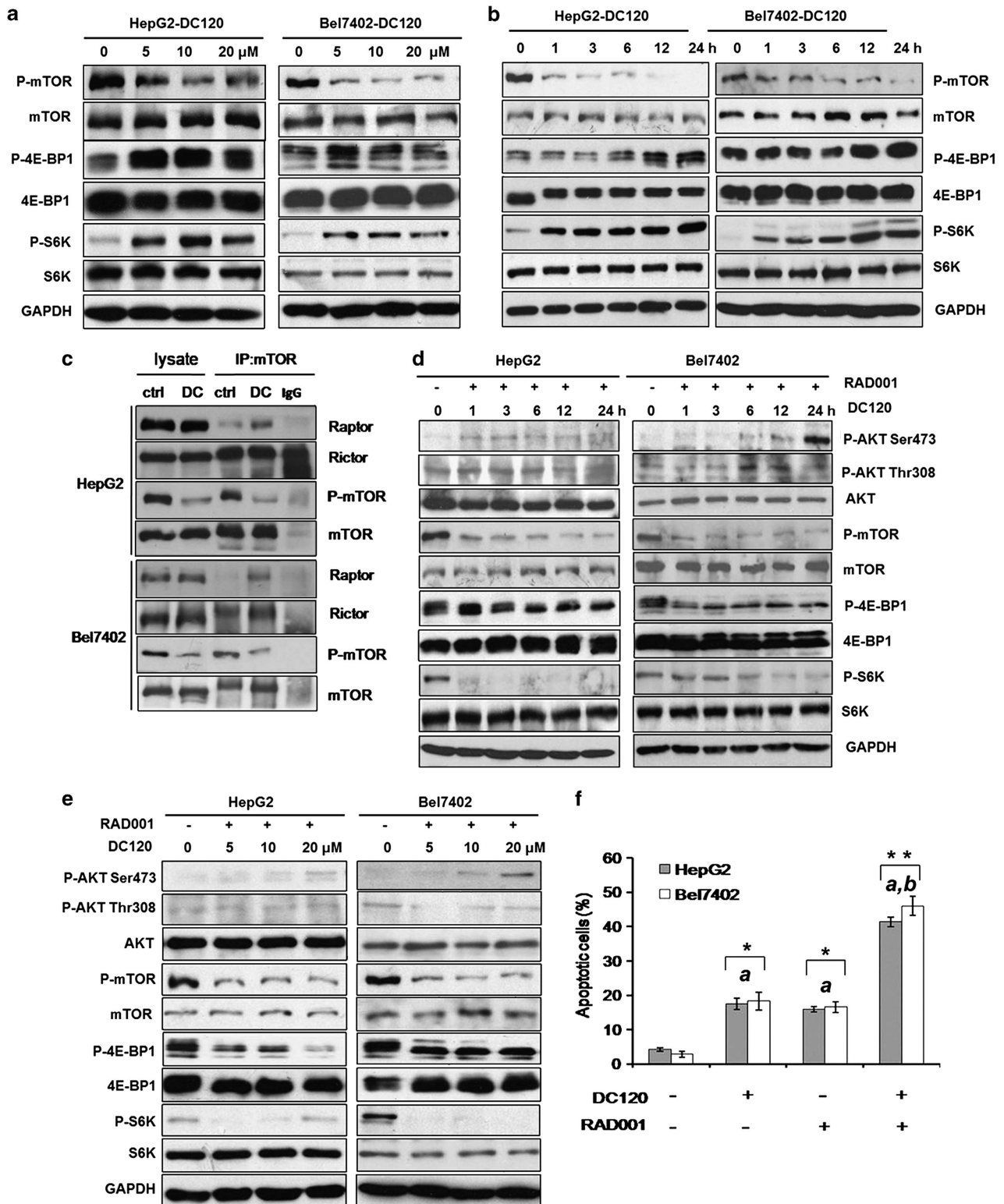
Figure 3 DC120 stimulated mTORC1 signaling and synergistically induced apoptosis with the mTORC1 inhibitor. (**a** and **b**) DC120 inhibited phosphorylation of mTOR but enhanced phosphorylation of P70S6K and 4E-BP1. (**c**) DC120 increased the binding of Raptor and mTOR but not Rictor and mTOR. Lysates were immunoprecipitated with the anti- mTOR antibody and the precipitates were probed with antibodies against mTOR, Rictor and Raptor. (**d** and **e**) The mTORC1 inhibitor RAD001 not only attenuated the phosphorylation of P70S6K and 4E-BP1 but also the phosphorylation of AKT at Thr308 and Ser473. (**f**) RAD001 sensitized cells to DC120-induced apoptosis. HepG2 and Bel7402 cells were pretreated with 1 μM RAD001 for 1 h followed by the addition of DC120 (10 μM) for another 48 h. *$P < 0.05$ *versus* the control, **$P < 0.01$ for the combination *versus* the control, DC120 alone and RAD001 alone, respectively; *a*, control; *b*, RAD001 alone or DC120 alone
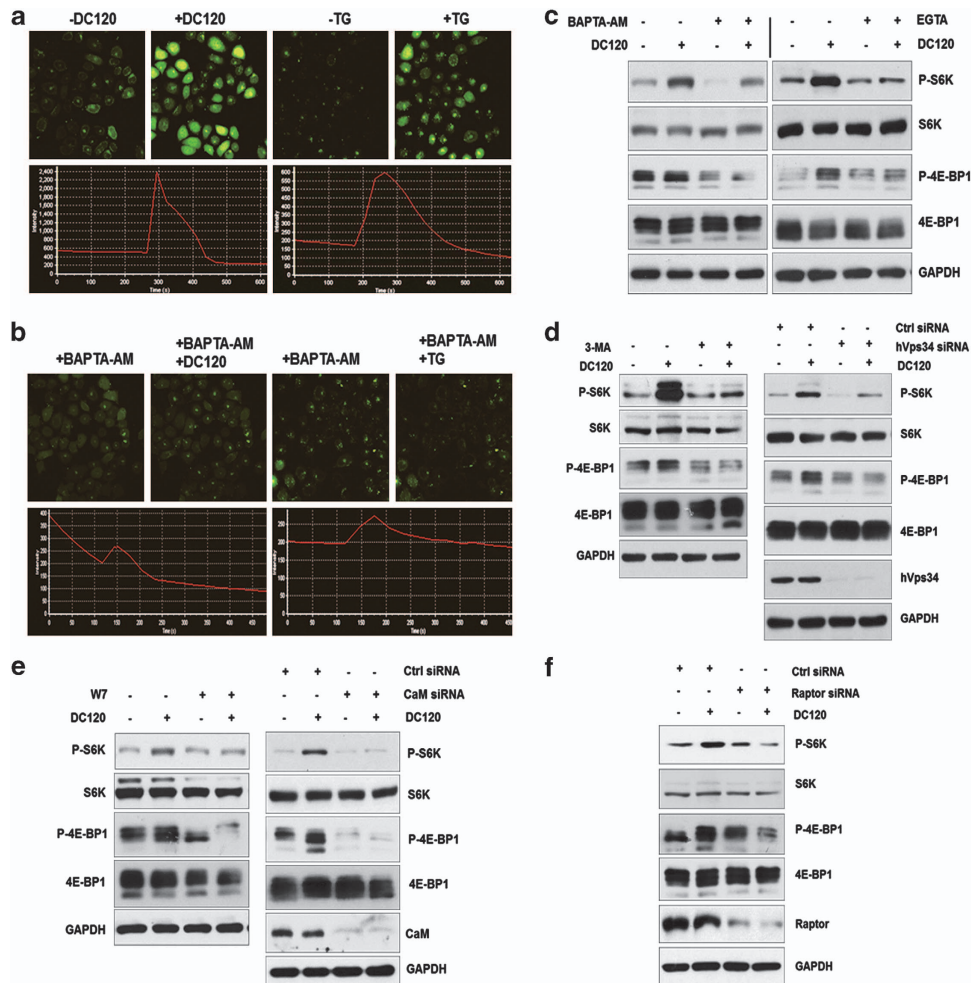
Figure 4 DC120 activated mTORC1 signaling via Ca^{2+}/CaM signaling to hVps34. (**a**)Treatment of DC120 induced an increase of intracellular Ca^{2+}. Bel7402 cells were treated with or without DC120 (10 μM) for 5 min in the absence of BAPTA-AM, images of TG (2 μM) as control. Upper panels present the confocal fluorescence images and lower panels are fluorescence intensity–time curves. (**b**) Ca^{2+} chelators reduced the increase of intracellular Ca^{2+} by DC120. Cells were treated with DC120 (10 μM) for 5 min or without DC120 in the preincubation of BAPTA-AM (2 μM), images of TG (2 μM) as control. (**c**) Ca^{2+} chelators selectively blocked mTORC1 signaling by DC120. Cells were pretreated with or without BAPTA-AM (20 μM) (left panel) or EGTA (5 μM) (right panel), then treated with or without DC120 (10 μM). (**d**) Increased intracellular Ca^{2+} induced mTORC1 signaling in an hVps34-dependent manner. Cells were pretreated with or without 3-MA (5 μM) (left panel). As in right panel, cells were transfected with either 100 nM Ctrl siRNA or 100 nM hVps34 siRNA. (**e**) CaM was required for hVps34 activity to mTORC1 signaling. Cells were pretreated with or without W7 (20 μM) (left panel). As in right panel, cells were transfected with either 50 nM Ctrl siRNA or a siRNA mix containing 15 nM each of CaM1, CaM2 and CaM3 siRNA. (**f**) Raptor knockdown blocked mTORC1 signaling by DC120. Cells were transfected with either 50 nM Ctrl siRNA or 50 nM Raptor siRNA

signaling. We also determined the phosphorylation of P70S6K and 4E-BP1 in AKT-depleted cells and found that P-S6K and P-4E-BP1 were decreased in AKT-depleted cells *versus* control cells (Supplementary Figure S5). Here, AKT knockdown inhibited the phosphorylation levels of S6K and 4E-BP1, which was consistent with a previous report.[16] However, the mechanism by which DC120 induced mTORC1 signaling was different from that of the AKT-depleted situation. Moreover, we observed an increase of binding of Raptor and mTOR upon treatment with DC120 compared with the control, but no obvious change of the binding of Rictor and mTOR (Figure 3c). These data were consistent with the activation of mTORC1 signaling by DC120 mentioned above.

RAD001 (Everolimus, the structure shown in Figure 1a) is a derivative of rapamycin and is functionally similar to rapamycin. RAD001 acts as an allosteric inhibitor of mTORC1, suppressing mTORC1 activity through its association with FK506 binding protein 12 (FKBP-12).[20–22] As shown in Figures 3d and e, RAD001 not only inhibited the phosphorylation of P70S6K and 4E-BP1 but also the phosphorylation of AKT Thr308 and Ser473. This suggested that hyperphosphorylation of AKT might be associated with mTORC1 activity. Furthermore, RAD001 sensitized DC120-induced apoptosis from 17.47 to 39.37% in HepG2 cells. Similarly, apoptosis was increased from 16.57 to 46.10% in Bel7402 cells treated with DC120 alone or in a combination of DC120 and RAD001, respectively (Figure 3f).

DC120 activated mTORC1 pathway via Ca^{2+}/CaM signaling to hVps34. To determine a permissive role for Ca^{2+} in DC120-mediated mTORC1 activation, intracellular

Ca^{2+} was measured by confocal microscopy with the Ca^{2+}-sensitive dye Fluo-3/AM.[23] As shown in Figure 4a, the treatment of DC120 evoked a rapid increase of intracellular Ca^{2+} that was similar to results observed with endoplasmic reticulum (ER) Ca^{2+}-ATPase inhibitor thapsigargin (TG)-induced increase of intracellular Ca^{2+}.[24] The intracellular Ca^{2+} increase in response to DC120 was rapidly reversed by preincubation with intracellular Ca^{2+} chelator BAPTA-acetoxymethyl ester (BAPTA-AM) (Figure 4b). When given DC120 at 5, 10 and 20 μM, we found that the increase of intracellular Ca^{2+} was dose dependent (Supplementary Figure S6A). Overexpression of AKT using plasmid HA-AKT attenuated the increase of intracellular Ca^{2+}, as shown in Supplementary Figure S6B, suggesting that the effect of DC120 on Ca^{2+} flux was dependent on AKT inhibition.

Furthermore, the pretreatment of Ca^{2+} chelators BAPTA-AM and ethylene glycol bis(2-aminoethyl) tetraacetic acid (EGTA) markedly suppressed DC120-mediated phosphorylation of P70S6K and 4E-BP1, indicating that activation of mTORC1 signaling by DC120 required intracellular Ca^{2+} (Figure 4c). It is not only specific for DC120-induced increase of Ca^{2+}, but also happens with other AKT inhibitors. GDC0068 also mediated increase of intracellular Ca^{2+} and, as shown in Supplementary Figure S7, the treatment of GDC0068 evoked a rapid increase of intracellular Ca^{2+}, and the intracellular Ca^{2+} increase by GDC0068 was rapidly reversed by preincubation with EGTA.

To explore how the increase of intracellular Ca^{2+} affected the mTORC1 pathway, we examined whether activation of P70S6K and 4E-BP1 by DC120 was sensitive to 3-methyladenine (3-MA), the hVps34 inhibitor. The results showed that DC120-induced phosphorylation of P70S6K and 4E-BP1 was abolished by pretreatment with 3-MA (Figure 4d, left panel). We also found that silencing of hVps34 by siRNAs blocked DC120-induced phosphorylation of P70S6K and 4E-BP1 (Figure 4d, right panel). These findings supported the model that Ca^{2+} mediated increased mTORC1 signaling by regulating hVps34 activity.

It was reported that Ca^{2+} could regulate hVps34 activity through CaM.[25] To test the potential role of Ca^{2+}/CaM in DC120-induced mTORC1 signaling, the cells were pretreated with N-(6-aminohexyl)-5-chloro-1-naphthalenesulfonamide (W7), a cell-permeable CaM antagonist that binds to CaM, thus preventing the binding of Ca^{2+}/CaM to target enzymes.[26] The results showed that pretreatment of Bel7402 cells with W7 blocked phosphorylation of P70S6K and 4E-BP1 following DC120 treatment (Figure 4e, left panel). In parallel, CaM silencing by a mixture of three distinct siRNAs against three distinct CaM genes blocked DC120-induced phosphorylation of P70S6K and 4E-BP1 (Figure 4e, right panel). Silencing of Raptor, the pivotal component of mTORC1, with siRNAs attenuated DC120-induced phosphorylation of P70S6K and 4E-BP1 and further confirmed the DC120-induced mTORC1 activation (Figure 4f). Together, these data suggested that Ca^{2+}/CaM/hVps34 was involved in DC120-mediated mTORC1 signaling.

DC120 activated MAPK pathway and synergistically induced apoptosis with the MEK inhibitor U0126. There is substantial cross-talk between PI3K/AKT and MEK/ERK

pathways, and the inhibition of either pathway leads to activation of the other one. Furthermore, AKT phosphorylates C-Raf Ser259 that leads to inhibition of the MEK/ERK pathway.[27] In our study, we noticed that DC120 constitutively activated the MEK/ERK pathway because of the inhibition of the AKT pathway in HepG2 and Bel7402 cells (Figures 5a and b), and we also detected ERK activation in AKT-depleted cells versus control cells (Supplementary Figure S5).

Moreover, as indicated in Figure 5c, DC120 markedly alleviated C-Raf Ser259 phosphorylation in dose- and time-dependent manners that suggested that the activation of MEK/ERK pathway was associated with the release of inhibitory C-Raf phosphorylation.

The compound U0126 was identified as a special inhibitor of MEK and its chemical structure is shown in Figure 1a.[28] We observed that U0126 blocked the phosphorylation of ERK1/2 even in the presence of DC120 in HepG2 and Bel7402 cells (Figure 5d). The data provided a mechanistic basis for the profound synergy of the combined inhibition of AKT and MEK pathways in tumors. As shown in Figure 5e, the MEK inhibitor U0126 sensitized DC120-induced apoptosis from 17.50% for treatment with 10 μM DC120 alone to 40.07% for combination treatment with 10 μM DC120 and 20 μM U0126 in HepG2 cells, and from 18.30 to 44.20% in Bel7402 cells under the same condition.

Antitumor activity of DC120 and its synergy with U0126 or RAD001 in vivo. To investigate the antitumor activity of DC120 in vivo, we established Bel7402 xenografts in nude mice. The tumor growth inhibitory rates were 37.5 and 56.7% in the 10 and 20 mg/kg DC120 groups, respectively (Figure 6a). Furthermore, DC120 in combination with U0126 or RAD001 synergistically suppressed tumor growth in xenograft models. The inhibitory rate of DC120 in combination with U0126 was 69.4 and 80.0% in combination with RAD001 (Figures 6b and c). In addition, we did not observe any toxicity in nude mice after treatment with DC120 alone or in combined treatments according to body weight measurement (Supplementary Figure S8).

The effect of DC120 on the AKT signaling in xenografts was consistent with the results of in vitro experiments (Figures 2a and b). DC120 also increased the phosphorylation of AKT but dramatically suppressed the phosphorylation of downstream substrates of AKT in vivo, including GSK3β, FOXO3α and PRAS40 (Figure 6d). Similarly, DC120 increased phosphorylation levels of P70S6K and 4E-BP1, and RAD001 alleviated the phosphorylation of P70S6K and 4E-BP1 in vivo (Figure 6e). ERK1/2 was also activated, and U0126 alleviated the phosphorylation of ERK1/2 in vivo (Figure 6f).

To determine whether growth inhibition by DC120 was caused by apoptosis, frozen sections of tumors were stained with transferase-mediated FITC-12-dUTP nick-end labeling (TUNEL) to identify the apoptotic cells. As shown in Supplementary Figure S9, there were no obvious TUNEL-positive cells in the control groups, whereas DC120 at 20 mg/kg stimulated a substantial increase in the number of TUNEL-positive cells. Significant numbers of TUNEL-positive cells were observed in the groups that received combination treatment of DC120 with RAD001 or U0126. These data
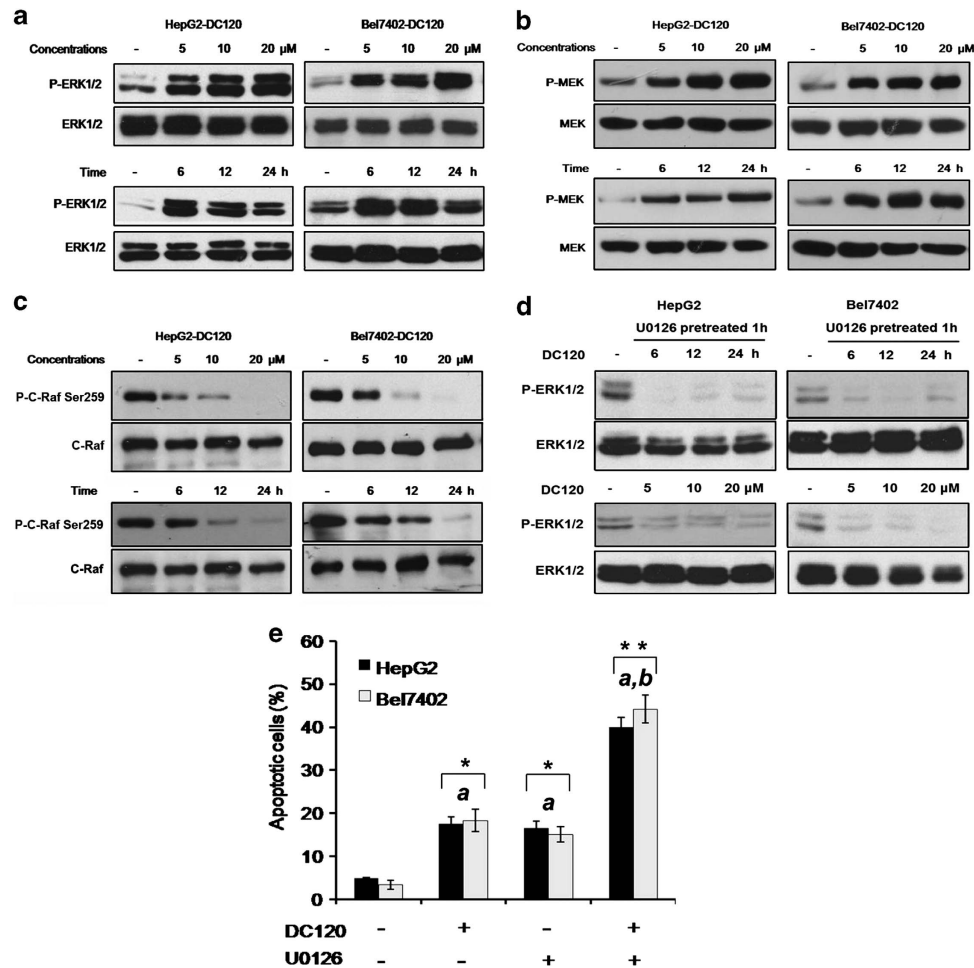
Figure 5 DC120 activated MAPK pathway and synergistically induced apoptosis with the MEK inhibitor. (**a** and **b**) DC120 constitutively activated the MEK/ERK pathway in dose- and time-dependent manners. (**c**) DC120 markedly decreased the phosphorylation of CRAF (Ser259) in dose- and time-dependent manners. (**d**) The MEK-specific inhibitor U0126 attenuated the stimulation of MEK/ERK pathway by DC120. Cells were pretreated with U0126 (20 μM) for 1 h and then treated with DC120 (10 μM). (**e**) U0126 sensitized cells to DC120-induced apoptosis. Cells were pretreated with U0126 (20 μM) for 1 h followed by the addition of DC120 (10 μM) for another 48 h. *$P < 0.05$ *versus* the control, **$P < 0.01$ for the combination *versus* the control, DC120 alone and U0126 alone, respectively; *a*, control; *b*, U0126 alone or DC120 alone

suggested that DC120 induced apoptosis and that the combination of DC120 with RAD001 or U0126 synergistically induced apoptosis *in vivo*.

Activation of MAPK and mTORC1 pathway following DC120 treatment was not mutually dependent. Increasing evidence shows that the MAPK and mTORC1 pathways are associated with each other. However, in our study, the MEK inhibitor U0126 did not block DC120-induced phosphorylation of P70S6K and 4E-BP1, and the mTORC1 inhibitor RAD001 did not alleviate the phosphorylation of ERK1/2 (Supplementary Figure S10A). These data showed that the activation of the two pathways was not mutually dependent following DC120 treatment. Therefore, the combination of these three inhibitors markedly increased the induction of apoptosis (Supplementary Figure S10B).

Discussion

The PI3K/AKT pathway is constitutively activated in many human malignancies including liver cancer, and it plays a

critical role in promoting tumor progression and resistance to treatment. In the present study, the novel AKT kinase inhibitor DC120 had strong specificity to the AKT kinase and low toxicity. DC120 suppressed proliferation and induced apoptosis through the inhibition of AKT kinase activity *in vitro* and *in vivo*. In particular, we showed that the AKT inhibitor relieved the feedback suppression of the mTORC1 and MAPK pathways. Thus, inhibition of these pathways sensitized AKT inhibitor-induced apoptosis *in vitro* and *in vivo*.

It is reported that binding of an inhibitor to the ATP site of AKT is sufficient to directly cause hyperphosphorylation of AKT without any stimulation through a conformational change templated by the inhibitor, such as A-443654 and GSK690693.[18,29] DC120 has completely different structure from A-443654 and GSK690693 and also induces AKT hyperphosphorylation (Figures 2a and b), which may be because of the above-mentioned conformational change by the inhibitor itself, at least partly. In addition, GDC0068, another new ATP-competitive AKT inhibitor that has a different structure from DC120, causes hyperphosphorylation of AKT (Supplementary Figure S4). These results
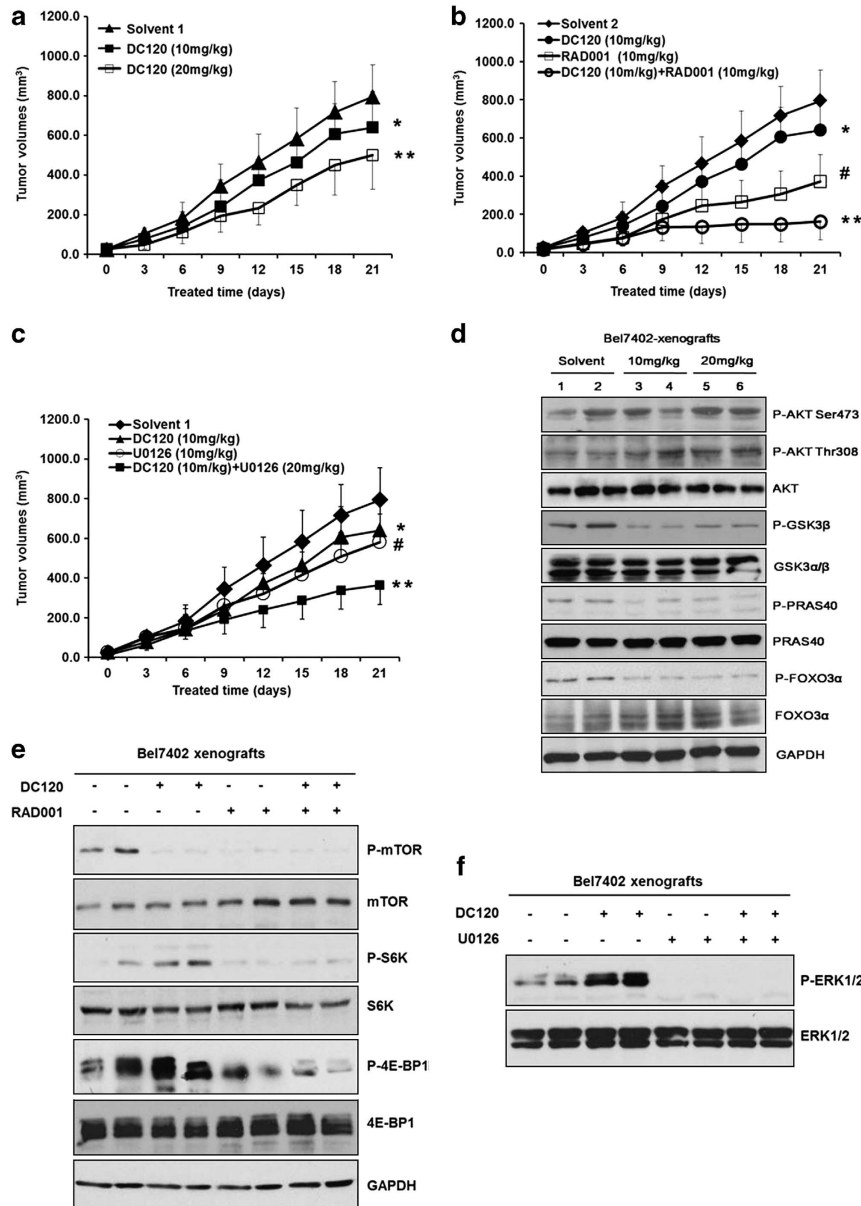
Figure 6 Antitumor activity of DC120 and its synergy with U0126 or RAD001 in vivo. (**a**) The antitumor efficacy of DC120. *$P < 0.025$ for DC120 10 mg/kg versus solvent 1, **$P < 0.025$ for DC120 20 mg/kg versus solvent 1. (**b**) Antitumor efficacy of DC120 in combination with RAD001. *$P < 0.0125$ for DC120 versus solvent 2; #$P < 0.0125$ for RAD001 versus solvent 2; **$P < 0.0125$ for combination versus solvent 2, RAD001 alone and DC120 alone. (**c**) Antitumor efficacy of DC120 in combination with U0126. *$P < 0.0125$ DC120 versus solvent 1; #$P < 0.0125$ U0126 versus solvent 1; **$P < 0.0125$ for combination versus solvent 1, DC120 alone and U0126 alone. (**d**) DC120 inhibited phosphorylation of AKT substrates and increased phosphorylation of AKT similarly in in vitro experiments. (**e**) RAD001 alleviated the phosphorylation of P70S6K and 4E-BP1 by DC120. (**f**) U0126 alleviated the phosphorylation of ERK1/2 by DC120

documented that the ATP-competitive AKT inhibitors have common points that cause hyperphosphorylation of AKT by the inhibitor itself when inhibiting AKT kinase activity. In contrast, AKT inhibition by MK2206, AKTi-1/2 and AKTi-1/2/3, which are non-ATP-competitive inhibitors, could block both AKT kinase activity and its phosphorylation level.[16,30]

Recently, the ribosome is identified as a missing link between PI3K and mTORC2, suggesting that the ribosome may be involved in mTORC2 activation.[31,32] Given that mTORC1 regulates ribosome biogenesis through the downstream substrate P70S6K, there may be an interplay between

the two mTOR complexes. Several studies have shown that the rapamycin-induced feedback activation of AKT (Thr308) is a consequence of the absence of P70S6K destabilization on the adaptor protein insulin receptor substrate-1 (IRS-1).[33,34] In our study, the AKT inhibitor DC120 increases mTORC1 activity that is reflected by the increased phosphorylation of 4E-BP1 and P70S6K (Figures 3a and b). DC120 induces the phosphorylation of P70S6K whose activity controls the ribosome biogenesis transcriptional program that promotes ribosome biogenesis and maturation, and therefore further activates the mTORC2 kinase.[35] AKT kinase activity is

suppressed following DC120 treatment, but AKT (Ser473) is phosphorylated by mTORC2, by which the above conformational change by the inhibitor itself contributes to the process, leading to the phosphorylation of AKT (Thr308). This is also consistent with the finding that the phosphorylation of AKT at both Ser473 and Thr308 is alleviated by the mTORC1 inhibitor RAD001 (Figure 3e). These data suggest that the mTORC1 pathway activates the mTORC2 pathway in a circuit that provides close interaction of the two complexes; the phosphorylation of AKT at Ser473 contributes to the phosphorylation of AKT at Thr308 that promotes the interaction of the two phosphorylated sites.

Various Ca^{2+}/ CaM-dependent signaling cascades with kinases and phosphatases often directly or indirectly influence cellular signals, including PI3K/AKT pathway, and recent reports also suggest that CaM/CaM-dependent protein kinase-II (CaMK-II) signaling can activate PI3K in monocytes.[36,37] However, Szado[8] has reported that AKT-mediated phosphorylation of IP3R resulted in a decrease in the magnitude of IP3-induced Ca^{2+} release and a resultant flux of Ca^{2+} from ER to mitochondria. Here, DC120 and GDC0068 induced an increase in intracellular Ca^{2+} (Figures 4a and b, Supplementary Figure S6A and Supplementary Figure S7) and we speculated that inhibition of AKT kinase by inhibitors dephosphorylated IP3R and led to flux of Ca^{2+} from ER to cytoplasm, which might be the common characteristics of ATP-competitive AKT inhibitors.

We observed the increase of intracellular Ca^{2+} that enhanced the binding of Ca^{2+}/CaM to hVps34, resulting in enhanced mTORC1 signaling with increased phosphorylation of P70S6K and 4E-BP1 (Figures 4c–e). Usually, hormones, growth factors and stress signals mediate mTORC1 activation through a canonical signaling cascade triggered by the activation of class I PI3K/AKT, leading to the sequential activation of the small GTPase Ras homolog enriched in brain (Rheb) and mTORC1.[38] In contrast, we found that mTORC1 signaling was stimulated by AKT inhibitor DC120 through Ca^{2+}/CaM cascades. DC120-induced activation of hVps34 leads to the increased production of PIP3 from phosphatidylinositol-3,4-bisphosphate (PIP2) that recruits AKT to plasma membrane again to activate AKT/mTOR signaling by feedback. The reactivation of AKT/mTOR signaling via Ca^{2+}/CaM in response to hVps34 is similar to amino acid-induced mTORC1 signaling, but contrary to insulin-induced survival associated with AKT/mTOR signaling.[39]

Many feedback loops and layers of cross-talk have been reported to connect the mTORC1, PI3K/AKT and MAPK pathways. The proximal mTORC1 activator Rheb is involved in direct inhibition of C-Raf activity and B-Raf/C-Raf heterodimerization that highlights the complexity of the connections among the mTORC1, PI3K/AKT and MAPK pathways.[40] However, inhibitory 14-3-3-binding sites on C-Raf (Ser259) can be phosphorylated by AKT and this phosphorylation inhibits the activation of the Raf/MEK/ERK signaling pathway.[27] In this study, DC120 relieved the inhibitory phosphorylation of C-Raf (Ser259) (Figure 5c) and thus activated the RAF/MEK/ERK signaling pathway. Nonetheless, the explicit mechanism of MAPK pathway activation by DC120 remains elusive. Other factors may be involved in this process, such as the overexpression and/or activation of receptor tyrosine

kinase (RTK), and should be further investigated. Chandarlapaty et al.[16] showed that AKT inhibition relieved the feedback suppression of RTK expression and activation, and induced the expression and phosphorylation of multiple RTKs, suggesting that the combined inhibition of AKT and HER kinase activity would be more effective than either alone.

Carriere et al.[41] reported that ERK1/2 phosphorylated Raptor to promote Ras-dependent activation of mTORC1. Another group suggested that the ERK and AKT signaling pathways function through parallel mechanisms to promote mTORC1 signaling.[42] Although accumulated evidence shows that MAPK pathway and mTOR pathway exhibit mutual crosstalk, our study shows that the two pathways are activated by DC120 in different mechanisms. They are not mutually dependent in their response to DC120 treatment. Therefore, the combined administration of DC120, RAD001 and U0126 would be a promising therapeutic strategy for liver cancer treatment.

Taken together, these data show that targeting AKT pathway alone is not sufficient to eradicate cancer. This is why some AKT inhibitors have initially entered clinical trials as components of a combination therapy, such as a combination of perifosine with radiotherapy and of MK-2206 with trastuzumab.[43] Here, we not only exploit a new compound targeting AKT kinase and clarify its antineoplastic mechanism, but also document the mechanisms by which the AKT inhibitor activates the mTORC1 and MAPK pathways, and report that the blockade of these feedback pathways potently sensitizes the antitumor activity of the AKT inhibitors on liver cancer in vitro and in vivo.

Materials and Methods

Cell lines. The human liver cell lines HepG2, SMMC7721, Bel7402 and Huh7 and human normal liver cell lines LO2 are cultured and conserved by Sun Yat-sen University Cancer Center and have been published before.[44–46] They are cultivated in Dulbecco's modified Eagle's medium supplemented with 10% fetal bovine serum in a humidified atmosphere containing 5% CO_2 at 37°C.

MTT assay. The method has been described elsewhere.[47] Absorbance values were measured at the wavelength of 570 nm. Inhibitory rates were calculated by Microsoft Excel and IC_{50} values were calculated using the Calcusyn software (Biosoft Corporation, Cambridge, UK).

Apoptosis assay. Propidium iodide (PI) staining was performed as described elsewhere.[48] Apoptosis was quantified by measuring the DNA content of cells by flow cytometry and the proportion of sub-G1-phase cells (%) represented the apoptosis rate. The identification of apoptotic cells using the Annexin V-FITC/PI staining method has also been described previously.[47] Annexin V-FITC-positive cells (%) represented early apoptotic cells, and Annexin V-FITC/PI-double-positive cells (%) represented dead cells.

Western blot analysis and immunoprecipitation. Cells were solubilized in lysis buffer. The protein concentration was determined using the Pierce BCA protein assay kit (Thermo Scientific Pierce, Rockford, IL, USA). Proteins were separated electrophoretically in SDS-polyacrylamide gels and transferred to PVDF membranes. The membranes were then blocked in a 5% skim milk solution in Tris-buffered saline containing 0.1% Tween (TBST) for 2 h and then incubated at 4°C overnight with a primary antibody, and subsequently incubated with HRP-conjugated secondary antibody at room temperature for 2 h. Immunoreactivity was detected using the Amersham ECL Prime Western Blot detection reagent (GE Healthcare, Fairfield, CT, USA) according to the manufacturer's instructions.

For immunoprecipitation, cells were lysed in ice-cold 0.3% CHAPS lysis buffer (40 mM HEPES (pH 7.4), 2 mM EDTA or 5 mM $MgCl_2$, 10 mM pyrophosphate,

10 mM glycerophosphate, 0.3% CHAPS or 1% Triton X-100, and one tablet of EDTA-free protease inhibitors (Roche, Branford, CT, USA) per 25 ml) for 1 h.[49] The whole-cell lysates were prepared by centrifugation at 13 000 r.p.m. and 4 °C for 30 min. The supernatant was removed and incubated with primary antibodies with rotation for 1–2 h at 4 °C. Then, 40 μl of 50% protein G-sepharose slurry was added per μg of lysate, and the rotation to mix continued for an additional 2 h or overnight at 4 °C. Immunoprecipitates were washed 3 times with 0.3% CHAPS lysis buffer and denatured by the addition of 20 μl 1 × SDS sample buffer and boiling for 5 min. Samples were isolated by 6–15% SDS-PAGE and analyzed by western blot. For AKT immunoprecipitation, the E1A lysis buffer (250 mM NaCl, 50 mM HEPES (pH 7.5), 0.1% NP-40, 5 mM EDTA, Roche protease inhibitor cocktail) was used,[50] and the experimental procedures were the same as those described above.

Retroviral DNA vectors, virus production and infection. The retroviral vector (pSUPER RNAi Puro, a gift of Professor Mu-Sheng Zeng, Cancer Center, Sun Yat-sen University, Guangzhou, China) encoding hairpin RNA sequences was constructed. The hairpin RNA (shRNA) sequences targeting Akt1 and PTEN were 5′-GAGTTTGAGTACCTGAAGCT-3′ and 5′-GGCGCUAUGU GUAUUAUUA-3′,[51] respectively. The shRNA primers were produced by Thermo Scientific Dharmacon (Rockford, IL, USA) according to the sequences we designed.

shRNA and siRNA transfection. Plasmid construction and virus production were performed as described elsewhere.[52] Transfection procedure was performed as described earlier.[47] The target sequences for hVps34-specific siRNA were hVps34 (920) 5′-ATGGCTGAAACTACCAGTAAA-3′ and hVps34 (923) 5′-ACGGTGATGAATCA TCTCCAA-3′,[53] siRNA sequences for CaM included CaM1, 5′-TTGCTAATAAGATACAACCAG-3′; CaM2, TACATATT GTT GAC TGTCCAT-3′ and CaM3, 5′-TTGGTGTTTGCTAGAACCGGG-3′.[39] The target sequence for Raptor-specific siRNA was 5′-GCGGAGAGCUCAUCAA CAATT-3′ and the control siRNA (Ctrl siRNA) sequence was 5′-UUCUCCGAAC GUGU CACGUTT-3′ (provided by GenChem Co. Shanghai, China), all of which were synthesized by GenChem Co.

Intracellular Ca^{2+} measurements. Bel7402 cells were seeded directly on special culture dishes and cultured for 24 h before treatment. After completely removing the medium, 200 μl Fluo-3/AM (5 μM) was added. The treated cells were then incubated for 45 min at 37 °C, 5% CO$_2$ humidified atmosphere. After removing Fluo-3/AM solution and washing with PBS twice, 1 ml PBS was left for intracellular Ca^{2+} measurements. Fluo-3/AM fluorescence intensity changes were determined by confocal microscopy. Images (excitation 488 nm, emission 525–530 nm) were acquired at 20 s intervals. Autofluorescence values were obtained at the end of each experiment.

Establishment of xenografts and in vivo study. Animal studies were performed in accordance with the criteria outlined in the 'Guide for the Care and Use of Laboratory Animals' prepared by the National Academy of Sciences and published by the National Institutes of Health (USA). Female BALB/C nude mice were purchased from Hunan Silaikejingda Laboratory Animal Technology Co. Ltd (Changsha, China). A total of 4×10^6 (0.2 ml) Bel7402 cells per mouse were inoculated subcutaneously into the right dorsal flanks of nude mice. When the tumors reached an average volume of ~0.1 cm^3, the mice were randomized into control and treated groups ($n = 6$ per group). The treatment groups received 10 mg/kg DC120, 20 mg/kg DC120, 10 mg/kg RAD001, 20 mg/kg U0126, a combination of 10 mg/kg DC120 and 10 mg/kg RAD001 or a combination of 10 mg/kg DC120 and 20 mg/kg U0126. The negative control groups received vehicle only, that is, NS, 4% (DMSO/Cremophor EL/ethanol = 1 : 2.1 : 0.9) dissolved in NS, called solvent 1, or 16% (DMSO/Cremophor EL/ethanol = 1 : 2.1 : 0.9) dissolved in NS, called solvent 2. The positive control group received 10 mg/kg CTX. DC120 and U0126 were solubilized in DMSO and then mixed with Cremophor EL, ethanol and NS in the same proportions as in solvent 1. RAD001 was solubilized in DMSO and then mixed with Cremophor EL, ethanol and NS in the same proportions as in solvent 2. DC120 and solvent 1 were administered by intraperitoneal injection once daily for 21 days. U0126 was administered by intraperitoneal injection, and RAD001 and solvent 2 were administered by intragastric administration once daily for 5 consecutive days each week for up to 21 days. CTX and NS were administered by intraperitoneal injection once weekly for up to 21 days. Tumor sizes were measured by caliper and recorded every 3 days. The tumor volumes were calculated from the length (the longest diameter across the tumor) and width (the corresponding perpendicular diameter) using the

following formula: $\pi/6 \times$ length $\times$ width^2. The tumor growth inhibitory rates were calculated as 100% × (1 − average size of treated tumor/size of control tumor) on each measurement day. Animal body weight was measured and recorded every 3 days during the treatment. On the day following the last dose, animals were killed and tumors were resected, preserved at − 80 °C for western blot and sectioned for the TUNEL assay.

Statistical analysis. The data were expressed as the means and S.E. Pairwise comparison was performed with the two-tailed Student's t-test, in which $P < 0.05$ was considered significant. Multiple comparisons were performed with Bonferroni correction and the two-tailed Student's t-test, in which $P < 0.05/N$ was considered significant, with N represented as times of comparisons.

Conflict of Interest

The authors declare no conflict of interest.

1. Jemal A, Bray F, Center MM, Ferlay J, Ward E, Forman D. Global cancer statistics. CA Cancer J Clin 2011; 61: 69–90.
2. Mitsui H, Takuwa N, Maruyama T, Maekawa H, Hirayama M, Sawatari T et al. The MEK1-ERK map kinase pathway and the PI 3-kinase-Akt pathway independently mediate anti-apoptotic signals in HepG2 liver cancer cells. Int J Cancer 2001; 92: 55–62.
3. Datta SR, Brunet A, Greenberg ME. Cellular survival: a play in three Akts. Genes Dev 1999; 13: 2905–2927.
4. Calleja V, Alcor D, Laguerre M, Park J, Vojnovic B, Hemmings BA et al. Intramolecular and intermolecular interactions of protein kinase B define its activation in vivo. PLoS Biol 2007; 5: e95.
5. Sarbassov DD, Guertin DA, Ali SM, Sabatini DM. Phosphorylation and regulation of Akt/PKB by the rictor-mTOR complex. Science 2005; 307: 1098–1101.
6. Manning BD, Cantley LC. AKT/PKB signaling: navigating downstream. Cell 2007; 129: 1261–1274.
7. Kim DH, Sarbassov DD, Ali SM, King JE, Latek RR, Erdjument-Bromage H et al. mTOR interacts with raptor to form a nutrient-sensitive complex that signals to the cell growth machinery. Cell 2002; 110: 163–175.
8. Szado T, Vanderheyden V, Parys JB, De Smedt H, Rietdorf K, Kotelevets L et al. Phosphorylation of inositol 1,4,5-trisphosphate receptors by protein kinase B/Akt inhibits Ca^{2+} release and apoptosis. Proc Natl Acad Sci USA 2008; 105: 2427–2432.
9. Soulsby MD, Wojcikiewicz RJ. The type III inositol 1,4,5-trisphosphate receptor is phosphorylated by cAMP-dependent protein kinase at three sites. Biochem J 2005; 392: 493–497.
10. Han EK, Leverson JD, McGonigal T, Shah OJ, Woods KW, Hunter T et al. Akt inhibitor A-443654 induces rapid Akt Ser-473 phosphorylation independent of mTORC1 inhibition. Oncogene 2007; 26: 5655–5661.
11. Levy DS, Kahana JA, Kumar R. AKT inhibitor, GSK690693, induces growth inhibition and apoptosis in acute lymphoblastic leukemia cell lines. Blood 2009; 113: 1723–1729.
12. Lin J, Sampath D, Nannini MA, Lee BB, Degtyarev M, Oeh J et al. Targeting activated Akt with GDC-0068, a novel selective Akt inhibitor that is efficacious in multiple tumor models. Clin Cancer Res 2013; 19: 1760–1772.
13. Liu R, Liu D, Trink E, Bojdani E, Ning G, Xing M. The Akt-specific inhibitor MK2206 selectively inhibits thyroid cancer cells harboring mutations that can activate the PI3K/Akt pathway. J Clin Endocrinol Metab 2011; 96: E577–E585.
14. Li Z, Oh DY, Nakamura K, Thiele CJ. Perifosine-induced inhibition of akt attenuates brain-derived neurotrophic factor/TrkB-induced chemoresistance in neuroblastoma in vivo. Cancer 2011; 117: 5412–5422.
15. Engelman JA, Chen L, Tan X, Crosby K, Guimaraes AR, Upadhyay R et al. Effective use of PI3K and MEK inhibitors to treat mutant Kras G12D and PIK3CA H1047R murine lung cancers. Nat Med 2008; 14: 1351–1356.
16. Chandarlapaty S, Sawai A, Scaltriti M, Rodrik-Outmezguine V, Grbovic-Huezo O, Serra V et al. AKT inhibition relieves feedback suppression of receptor tyrosine kinase expression and activity. Cancer Cell 2011; 19: 58–71.
17. Deng R, Yang F, Chang SH, Tang J, Qin J, Feng GK et al. DC120, a novel and potent inhibitor of AKT kinase, induces tumor cell apoptosis and suppresses tumor growth. Mol Pharmacol 2012; 82: 189–198.
18. Okuzumi T, Fiedler D, Zhang C, Gray DC, Aizenstein B, Hoffman R et al. Inhibitor hijacking of Akt activation. Nat Chem Biol 2009; 5: 484–493.

19. Ma XM, Blenis J. Molecular mechanisms of mTOR-mediated translational control. *Nat Rev Mol Cell Biol* 2009; **10**: 307–318.

20. Sedrani R, Cottens S, Kallen J, Schuler W. Chemical modification of rapamycin: the discovery of SDZ RAD. *Transplant Proc* 1998; **30**: 2192–2194.

21. Choi J, Chen J, Schreiber SL, Clardy J. Structure of the FKBP12-rapamycin complex interacting with the binding domain of human FRAP. *Science* 1996; **273**: 239–242.

22. Zhou HY, Huang SL. Current development of the second generation of mTOR inhibitors as anticancer agents. *Chin J Cancer* 2012; **31**: 8–18.

23. Tretyn A, Kado RT, Kendrick RE. Loading and localization of Fluo-3 and Fluo-3/AM calcium indicators in sinapis alba root tissue. *Folia Histochem Cytobiol* 1997; **35**: 41–51.

24. Thastrup O, Cullen PJ, Drobak BK, Hanley MR, Dawson AP. Thapsigargin, a tumor promoter, discharges intracellular Ca^{2+} stores by specific inhibition of the endoplasmic reticulum Ca^{2+}-ATPase. *Proc Natl Acad Sci USA* 1990; **87**: 2466–2470.

25. Vergne I, Chua J, Deretic V. Tuberculosis toxin blocking phagosome maturation inhibits a novel Ca^{2+}/calmodulin-PI3K hVPS34 cascade. *J Exp Med* 2003; **198**: 653–659.

26. Kahl CR, Means AR. Regulation of cell cycle progression by calcium/ calmodulin-dependent pathways. *Endocr Rev* 2003; **24**: 719–736.

27. Zimmermann S, Moelling K. Phosphorylation and regulation of Raf by Akt (protein kinase B). *Science* 1999; **286**: 1741–1744.

28. Favata MF, Horiuchi KY, Manos EJ, Daulerio AJ, Stradley DA, Feeser WS et al. Identification of a novel inhibitor of mitogen-activated protein kinase kinase. *J Biol Chem* 1998; **273**: 18623–18632.

29. Heerding DA, Rhodes N, Leber JD, Clark TJ, Keenan RM, Lafrance LV et al. Identification of 4-(2-(4-amino-1,2,5-oxadiazol-3-yl)-1-ethyl-7-{[(3S)-3- piperidinylmethyl]oxy}-1H- imidazo[4,5-c]pyridin-4-yl)-2-methyl-3-butyn-2-ol (GSK690693), a novel inhibitor of AKT kinase. *J Med Chem* 2008; **51**: 5663–5679.

30. Sangai T, Akcakanat A, Chen H, Tarco E, Wu Y, Do KA. Biomarkers of response to Akt inhibitor MK-2206 in breast cancer. *Clin Cancer Res* 2012; **18**: 5816–5828.

31. Zinzalla V, Stracka D, Oppliger W, Hall MN. Activation of mTORC2 by association with the ribosome. *Cell* 2011; **144**: 757–768.

32. Xie X, Guan KL. The ribosome and TORC2: collaborators for cell growth. *Cell* 2011; **144**: 640–642.

33. Shah OJ, Hunter T. Turnover of the active fraction of IRS1 involves raptor- mTOR- and S6K1-dependent serine phosphorylation in cell culture models of tuberous sclerosis. *Mol Cell Biol* 2006; **26**: 6425–6434.

34. Shah OJ, Wang Z, Hunter T. Inappropriate activation of the TSC/Rheb/mTOR/ S6K cassette induces IRS1/2 depletion, insulin resistance, and cell survival deficiencies. *Curr Biol* 2004; **14**: 1650–1656.

35. Chauvin C, Koka V, Nouschi A, Mieulet V, Hoareau-Aveilla C, Dreazen A et al. Ribosomal protein S6 kinase activity controls the ribosome biogenesis transcriptional program. *Oncogene* 2013; **33**: 474–483.

36. Ma W, Mishra S, Gee K, Mishra JP, Nandan D, Reiner NE et al. Cyclosporin A and FK506 inhibit IL-12p40 production through the calmodulin/calmodulin- dependent protein kinase-activated phosphoinositide 3-kinase in lipopolysaccharide- stimulated human monocytic cells. *J Biol Chem* 2007; **282**: 13351–13362.

37. Yano S, Tokumitsu H, Soderling TR. Calcium promotes cell survival through CaM-K kinase activation of the protein-kinase-B pathway. *Nature* 1998; **396**: 584–587.

38. Dann SG, Selvaraj A, Thomas G. mTOR Complex1-S6K1 signaling: at the crossroads of obesity, diabetes and cancer. *Trends Mol Med* 2007; **13**: 252–259.

39. Gulati P, Gaspers LD, Dann SG, Joaquin M, Nobukuni T, Natt F et al. Amino acids activate mTOR complex 1 via Ca^{2+}/CaM signaling to hVps34. *Cell Metab* 2008; **7**: 456–465.

40. Karbowniczek M, Robertson GP, Henske EP. Rheb inhibits C-raf activity and B-raf/C-raf heterodimerization. *J Biol Chem* 2006; **281**: 25447–25456.

41. Carriere A, Romeo Y, Acosta-Jaquez HA, Moreau J, Bonneil E, Thibault P et al. ERK1/2 phosphorylate Raptor to promote Ras-dependent activation of mTOR complex 1 (mTORC1). *J Biol Chem* 2011; **286**: 567–577.

42. Winter JN, Jefferson LS, Kimball SR. ERK and Akt signaling pathways function through parallel mechanisms to promote mTORC1 signaling. *Am J Physiol Cell Physiol* 2011; **300**: C1172–C1180.

43. Pal SK, Reckamp K, Yu H, Figlin RA. Akt inhibitors in clinical development for the treatment of cancer. *Expert Opin Investig Drugs* 2010; **19**: 1355–1366.

44. Liu L, Zhang CZ, Cai M, Fu J, Chen GG, Yun J. Downregulation of polo-like kinase 4 in hepatocellular carcinoma associates with poor prognosis. *PLoS One* 2012; **7**: e41293.

45. Zhao JJ, Pan K, Li JJ, Chen YB, Chen JG, Lv L et al. Identification of LZAP as a new candidate tumor suppressor in hepatocellular carcinoma. *PLoS One* 2011; **6**: e26608.

46. Xu S, Feng Z, Zhang M, Wu Y, Sang Y, Xu H et al. hSSB1 binds and protects p21 from ubiquitin-mediated degradation and positively correlates with p21 in human hepatocellular carcinomas. *Oncogene* 2011; **30**: 2219–2229.

47. Deng R, Li W, Guan Z, Zhou JM, Wang Y, Mei YP et al. Acetylcholinesterase expression mediated by c-Jun-NH2-terminal kinase pathway during anticancer drug-induced apoptosis. *Oncogene* 2006; **25**: 7070–7077.

48. Zhang XD, Borrow JM, Zhang XY, Nguyen T, Hersey P. Activation of ERK1/2 protects melanoma cells from TRAIL-induced apoptosis by inhibiting Smac/DIABLO release from mitochondria. *Oncogene* 2003; **22**: 2869–2881.

49. Sancak Y, Bar-Peled L, Zoncu R, Markhard AL, Nada S, Sabatini DM. Ragulator- Rag complex targets mTORC1 to the lysosomal surface and is necessary for its activation by amino acids. *Cell* 2010; **141**: 290–303.

50. Yang WL, Wang J, Chan CH, Lee SW, Campos AD, Lamothe B et al. The E3 ligase TRAF6 regulates Akt ubiquitination and activation. *Science* 2009; **325**: 1134–1138.

51. Sze KM, Wong KL, Chu GK, Lee JM, Yau TO, Ng IO. Loss of phosphatase and tensin homolog enhances cell invasion and migration through AKT/Sp-1 transcription factor/ matrix metalloproteinase 2 activation in hepatocellular carcinoma and has clinicopathologic significance. *Hepatology* 2011; **53**: 1558–1569.

52. Deng R, Tang J, Ma JG, Chen SP, Xia LP, Zhou WJ et al. PKB/Akt promotes DSB repair in cancer cells through upregulating Mre11 expression following ionizing radiation. *Oncogene* 2011; **30**: 944–955.

53. Nobukuni T, Joaquin M, Roccio M, Dann SG, Kim SY, Gulati P et al. Amino acids mediate mTOR/raptor signaling through activation of class 3 phosphatidylinositol 3OH-kinase. *Proc Natl Acad Sci USA* 2005; **102**: 14238–14243.

Supplementary Information accompanies this paper on Cell Death and Disease website (http://www.nature.com/cddis)